Progress In Electromagnetics Research C, Vol. 121, 265–279, 2022

Multiband Compact MIMO Antenna for Cognitive Radio, IoT and 5G New Radio Sub 6 GHz Applications

Bisma Bukhari* **and Ghulam M. Rather**

Abstract—A planar, handheld device size compatible, multiple-input multiple-output (MIMO) antenna design is proposed. The antenna system has five antennas which cover multiple wireless bands. One pair of elements covers the frequencies below 1 GHz (559 MHz to 828 MHz) for Long term evolution (LTE) and Cognitive radio (CR) applications and frequency bands 1.68 GHz to 1.77 GHz, 2.48 GHz to 2.63 GHz, 3.3 GHz to 3.4 GHz, and 5.79 GHz to 6 GHz for Internet of Things (IoT). The other pair is a modified truncated tetrahedron wideband antenna which covers multiple bands like 854 MHz to 958 MHz, 1.38 GHz to 1.56 GHz, 1.75 GHz to 1.87 GHz, 2.08 GHz to 2.49 GHz, 3.29 GHz to 3.47 GHz, and 4.09 GHz to 6 GHz including the triple radio frequency identification (RFID) bands. The antenna is designed and simulated using CST microwave studio simulator, and antenna prototype is fabricated to obtain the experimental results.

1. INTRODUCTION

Evolving technologies pave the way for Next Generation applications which have enormous capacity and portability needs. These applications need wide bandwidth to cover multiple frequency bands [1–3]. As the spectrum remains unused most of the time, a promising approach to tackle the issue of idle and underutilized spectrum is Cognitive Radio (CR) [4]. CR enhances the spectrum efficiency and minimizes over crowdedness by using the spectrum which is idle and unoccupied by the primary user at that time. By doing so, it efficiently manages the access to the spectrum (Dynamic Spectrum Management) for various wireless applications [5]. To improve the reliability, data rates, and range in a CR system, it is essential to implement MIMO configuration in the antenna system [6]. The implementation of MIMO-based cognitive radio devices ensures a reliable wireless link between the users while providing a good spectrum efficiency [7–9]. It also ensures a good quality of service to various wireless technologies like Wi-Fi, long term evolution (LTE), 5G, etc. [10]. Nowadays, due to the scaling down of the circuit and integration of different functionalities in a wireless device, there is an extensive growth in various wireless communication standards like LTE technology which offers high data rates [11–18]. So, one of the design challenges is to design a compact MIMO antenna system to cover various LTE bands especially the lower frequency bands below 1 GHz such as LTE 700 because there is an inverse relationship between the antenna size and its frequency of operation. In addition to cognitive radio and MIMO, the demand for Internet-of-Things (IoT) has increased tremendously due to its application in healthcare, logistics, transportation, tracking, etc., which involve the use of radio frequency identification (RFID) techniques [19–21]. The important frequency bands used by RFID include ultra-high frequency (840 MHz to 960 MHz), microwave frequency (2.4 GHz to 2.48 GHz), and super-high frequency (5.72 GHz to 5.87 GHz) bands depending on the application [22]. For an automated RFID system and its integration with multiple wireless standards, designing multiband and multistandard antennas is extremely important. Previously, multiple antennas were designed for

Received 18 May 2022, Accepted 21 July 2022, Scheduled 1 August 2022
* Corresponding author: Bisma Bukhari (bismabukhari11@gmail.com).
The authors are with the Department of Electronics and Communication Engineering, NIT Srinagar, J&K, 190006, India.

different applications which increased the overall size of the wireless system. Nowadays, due to the miniaturization of devices, multiple compact antennas need to be designed on a limited space, and these compact antennas should be able to cover multiple bands while providing optimum antenna performance [3, 7]. Until now, many new antenna designs have been developed for handheld devices; however as the devices become noticeably small in size, the requirements regarding efficiency and bandwidth have become greater than before, particularly with more up to date LTE Standards, where the antenna has to work over wide frequency range from as low as 700 MHz up to a few Gigahertz [10, 13, 21, 22]. The real challenge is the antenna design for the low and high ends of the spectrum. Since the size of the antenna has to be increased for the lower frequencies, it becomes unsuitable for the handheld gadgets. Other issues include the coupling between antennas and current localization when the antenna elements are integrated on the same substrate. MIMO antennas for LTE standard are presented in [11–18] which cover multiple bands for various applications in 4G LTE, GSM 900, WLAN, etc. The drawbacks of above antennas are that the DGS and via holes used in them change the impedance matching of MIMO antennas which in turn affect the antenna performance. To minimize coupling, slots are incorporated on ground, and additional ground extensions are added. The addition of extra arms and ground extensions makes the circuits more complex and introduce undesired parasitic resonances. CR antennas implemented in single-input single-output (SISO) configurations are presented in [23–29] where the antenna systems comprise a wideband antenna and a narrowband antenna. An external tuning circuit is used for tuning the narrowband antenna which makes the design more complex. Also, the isolation between antenna elements is very poor which degrades the performance. In some of the antenna designs, a stepper motor is used for tuning the reconfigurable antenna which makes the antenna system extremely bulky. Also, the sensing range is very small, and they do not cover lower frequencies below 1 GHz. For increasing the channel capacity, the MIMO implementation of CR is in great demand [32]. Some of these works are reported in [34–36]. Though these antennas cover multiple bands, most of them are unable to cover lower frequency bands below 1 GHz and some useful sub 6 GHz bands while others have extremely small sensing and communication ranges. Also, majority of the works only investigated the radiation characteristics while ignoring important antenna performance parameters like gain, directivity, and other MIMO characteristics like envelope correlation coefficient (ECC), etc. An important design challenge is to cover multiple wireless standards like MIMO, CR, IoT, and RFID applications while maintaining optimal antenna performance. To improve the data rates of the antenna and to make it compatible with multiple wireless standards like IoT, CR, LTE, and radio frequency identification (RFID), a novel, MIMO antenna system having five-elements is proposed. It is designed using an FR-4 substrate having size 65 mm × 120 mm × 1.6 mm. The MIMO antenna system is made up of following antennas:

1) Antenna 1 which not only is a ground plane for other antenna elements, but can also be used as a wideband sensing antenna to cover bands like 0.78 GHz to 1.07 GHz, 1.36 GHz to 1.6 GHz, 2.07 GHz to 2.93 GHz, 5.21 GHz to 5.36 GHz, and 5.54 GHz to 6 GHz.

2) Antennas 2 and 3 which operate over bands like 559 MHz to 828 MHz, 1.68 GHz to 1.77 GHz, 2.48 GHz to 2.63 GHz, 3.3 GHz to 3.4 GHz, and 5.79 GHz to 6 GHz and thus cover the LTE 700 MHz for CR, 4G, etc.

3) Antennas 4 and 5 with a modified truncated tetrahedron topology to cover 854 MHz to 958 MHz, 1.38 GHz to 1.56 GHz, 1.75 GHz to 1.87 GHz, 2.08 GHz to 2.49 GHz, 3.29 GHz to 3.4 GHz, and 4.09 GHz to 6 GHz bands for multiple wireless communication platforms including IoT for RFID applications.

The proposed design is simulated using CST simulator and then fabricated for obtaining experimental values. Important MIMO performance parameters like realized gain and ECC are also evaluated experimentally. The paper comprises six sections. Section 2 shows the proposed MIMO antenna design. Section 3 gives the measured values of the fabricated antenna. Section 4 shows the experimental and simulated MIMO parameters like realized gain and ECC. Section 5 presents the state-of-art comparison of the proposed design with some of the related works, and Section 6 gives the conclusion.

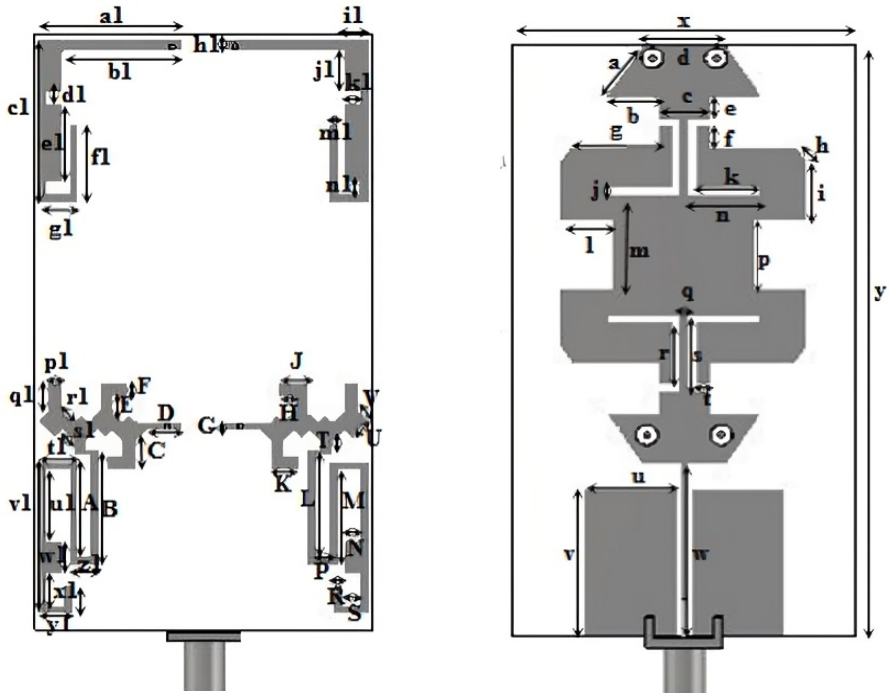

(a) (b)

Figure 1. Proposed MIMO antenna. (a) Front view. (b) Back view.

2. PROPOSED MIMO ANTENNA DESIGN

The proposed design is fabricated using an FR-4 substrate ($\tan\delta = 002$ and $\varepsilon_r = 44$) as shown in Fig. 1, having size 65 mm × 120 mm × 1.6 mm due to which it can be used in small portable devices. The top of the substrate consists of four antenna elements (antenna 2–antenna 5) at four corners. The bottom of the substrate consists of antenna 1 which serves as not only a ground for these antenna elements but also a sensing antenna since it has its separate coplanar ground. Antennas 2 and 3 operate in LTE 700 MHz band along with some important wireless bands needed in CR Antennas 4 and 5 which are designed for higher frequencies needed for IoT and RFID applications. Since the sensing antenna (antenna 1) has a separate ground plane, it can independently cover some additional important frequencies from 0.559 GHz to 6 GHz. MIMO antenna dimensions are given in Table 1.

2.1. Sensing Antenna

Antenna 1 acts as a ground as well a sensing antenna. Initial design approach involves the equivalent area technique [3] for covering a wide sensing range. The resonant frequency is given by [3]:

$$f_r = \frac{7.2}{\{(L+p+r)\times k\}}\,\text{GHz} \tag{1}$$

where L, p, r, and k denote patch length, feed distance from ground (in cm), feed radius, and dielectric constant's effect on lower frequency, respectively. The antenna is then modified by tapering the edges as shown in Fig. 2(a) so that more space is available for accommodating multiple antennas for CR applications and efficient implementation of MIMO. The antenna operates in the frequency bands like 0.78 GHz to 1.07 GHz, 1.36 GHz to 1.6 GHz, 2.07 GHz to 2.93 GHz, 5.21 GHz to 5.36 GHz, and 5.54 GHz to 6 GHz. To cover the lower frequencies, the size of antenna has to be increased which is not feasible keeping in view the size constraints. So, in order to cover the lower frequency bands like LTE 700 MHz band, slots are incorporated in sensing antenna as shown in Fig. 2(b). Slots help in increasing the path of the surface current which in turn lowers the frequency. Fig. 2(c) gives the S_{11} parameters of the slotted and the unslotted antenna which shows a downward shift in frequency of the slotted patch.

Table 1. Antenna design parameters.

Parameter	Size (mm)	Parameter	Size (mm)	Parameter	Size (mm)	Parameter	Size (mm)
a	12.52	s	15	$k1$	3	C	6
b	9.89	t	3	$l1$	6	D	6.8
c	10	u	17.65	$m1$	2	E	3
d	16	v	30	$n1$	2	F	3
e	4.54	w	35	$p1$	2.8	G	2
f	4.46	x	65	$q1$	6	H	3
g	16.47	y	120	$r1$	3	J	5.8
h	3.7	$a1$	28	$s1$	3	K	5.8
i	11.91	$b1$	23	$t1$	8	L	20.3
j	1	$c1$	33	$u1$	14	M	19
k	12	$d1$	2	$v1$	31	N	3
l	10	$e1$	16	$w1$	7	P	2
m	19.46	$f1$	16	$x1$	6	R	2
n	13	$g1$	8	$y1$	7	S	3
p	14	$h1$	2.5	$z1$	6	T	2.7
q	2	$i1$	5	A	19	U	4.7
r	13	$j1$	8.5	B	23.5	V	2.7

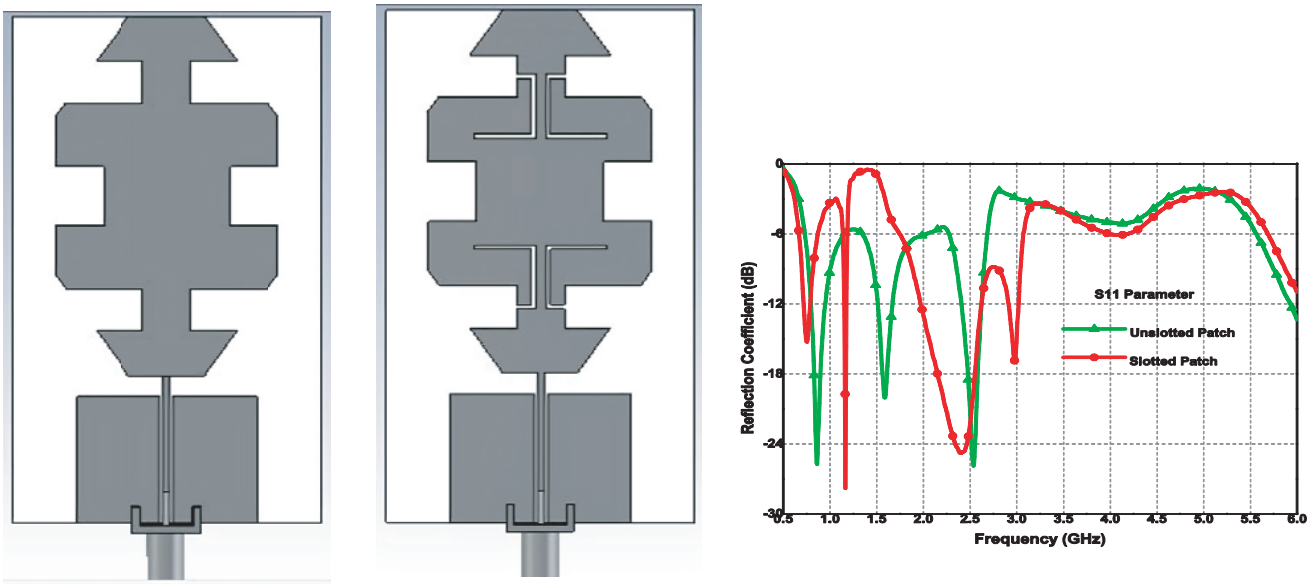

(a) (b) (c)

Figure 2. Antenna 1. (a) Unslotted, (b) Slotted and (c) Simulated S_{11} response.

2.2. Lower LTE Band Antenna

At the top corners of the substrate, two modified meandered antennas are placed. The initial design approach involved the design of a $\lambda/4$ meandered antenna (antenna 2), where λ denotes the antenna wavelength at 0.7 GHz. This antenna is then modified to improve the impedance matching. The

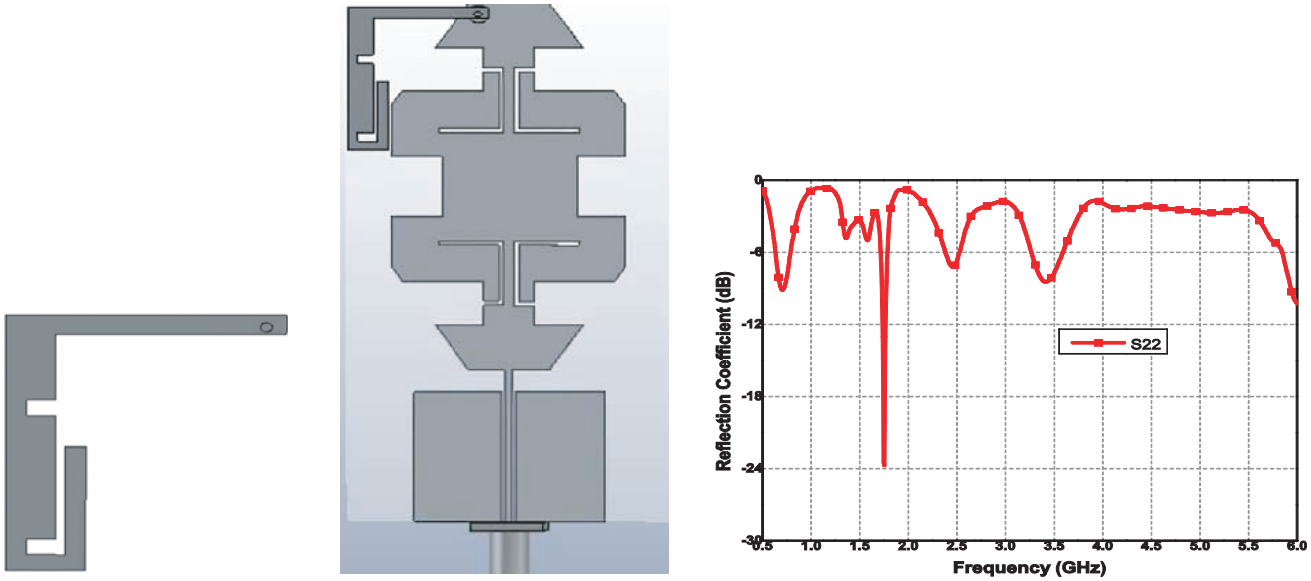

(a) (b) (c)

Figure 3. Antenna 2. (a) Topology, (b) Connection with ground plane and (c) Simulated S_{22} response.

modified design helps in reducing the lower frequency which is desirable for operating in lower LTE bands. Fig. 3(a), Fig. 3(b), and Fig. 3(c) show the proposed LTE band antenna, its connection with ground, and its S_{22} response, respectively. The antenna follows the -6 dB matching criterion and covers the lower frequencies below 1 GHz (559 MHz to 828 MHz) for Long term evolution (LTE) and Cognitive radio (CR) applications. In addition to these bands, it also covers frequencies from 1.68 GHz to 1.77 GHz, 2.48 GHz to 2.63 GHz, 3.3 GHz to 3.4 GHz, 5.79 GHz to 6 GHz for IoT and RFID applications due to generation of higher order modes.

2.3. High-Frequency Wideband Antenna

The antenna as shown in Fig. 4(a) is an Archimedean structure [37] having a high symmetry. To cover multiple bands, there is a requirement of large bandwidth. The proposed design shown in Fig. 4(b) is a wideband modified planar truncated tetrahedron in which the bandwidth is increased by loading stubs in it. The S-parameters with different stub sections (1 to 4) and without stub section are given in Fig. 4(c). The antenna operates over a wide band of frequencies like 854 MHz to 958 MHz, 1.38 GHz to 1.56 GHz, 1.75 GHz to 1.87 GHz, 2.08 GHz to 2.49 GHz, 3.29 GHz to 3.47 GHz, and 4.09 GHz to 6 GHz which include triple RFID bands of 858 MHz to 930 MHz, 2.4 GHz to 2.45 GHz, and 5.72 GHz to 5.87 GHz.

2.4. MIMO Implementation

MIMO improves the data rates, reliability, and range in a cognitive radio system. Fig. 1 shows the proposed MIMO implementation. When all MIMO elements are integrated on a common ground, coupling takes place which changes the overall S-parameters of the individual antennas as given in Fig. 5(a). The plot shows that antennas 2 and 3 cover the frequencies like 559 MHz to 828 MHz, 1.68 GHz to 1.77 GHz, 2.48 GHz to 2.63 GHz, 3.3 GHz to 3.4 GHz, and 5.79 GHz to 6 GHz. Antenna 4 and 5 cover multiple bands like 854 MHz to 958 MHz, 1.38 GHz to 1.56 GHz, 1.75 GHz to 1.87 GHz, 2.08 GHz to 2.49 GHz, 3.29 GHz to 3.47 GHz, and 4.09 GHz to 6 GHz. Sensing antenna 1 covers 0.78 GHz to 1.07 GHz, 1.36 GHz to 1.6 GHz, 2.07 GHz to 2.93 GHz, 5.21 GHz to 5.36 GHz, and 5.54 GHz to 6 GHz frequency bands. Fig. 5(b) shows the isolation between antenna elements. For antennas 2 and 3, isolation (S_{23}) at frequencies below 1 GHz is above 10 dB. Though antennas 4 and 5 also cover the frequencies below 1 GHz, the isolation (S_{45}) is poor. Therefore, for frequencies below 1 GHz like LTE

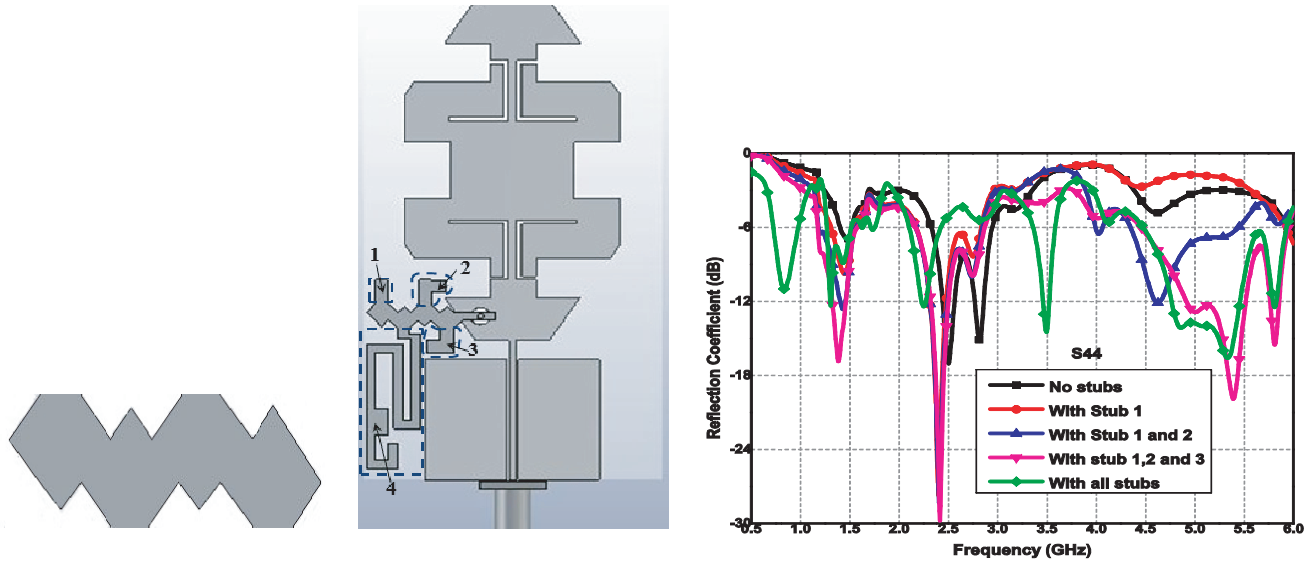

(a) (b) (c)

Figure 4. Antenna 3. (a) Truncated tetrahedron, (b) Modified truncated tetrahedron and (c) Reflection coefficient.

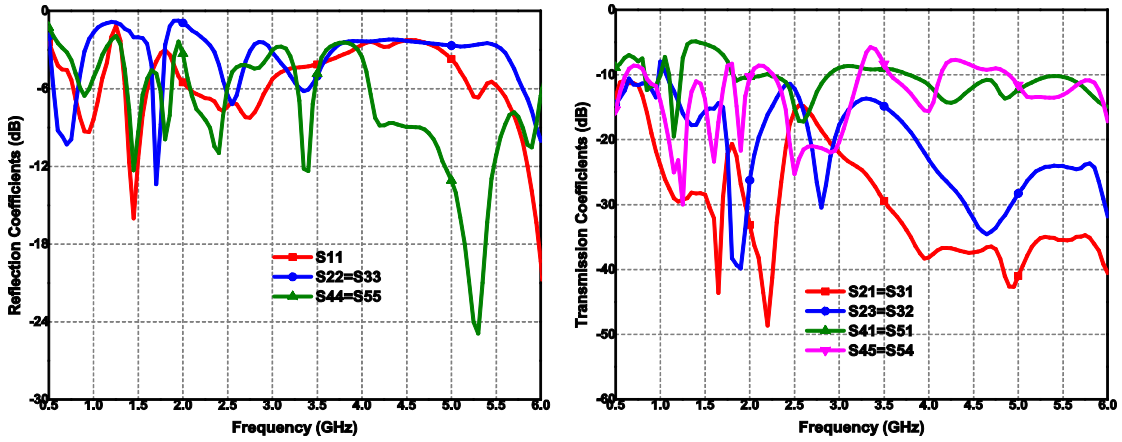

(a) (b)

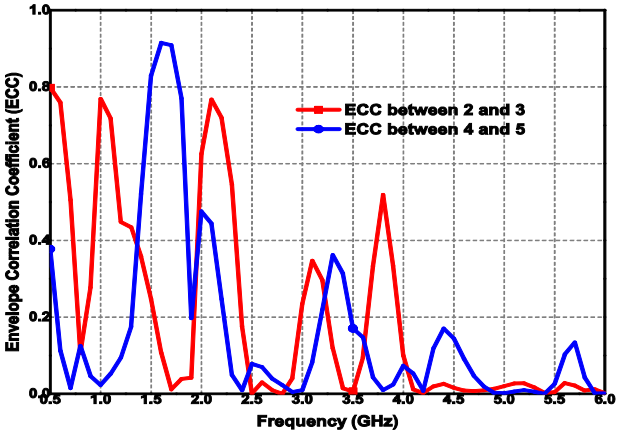

(c)

Figure 5. (a) Reflection coefficients, (b) transmission coefficients and (c) envelope correlation coefficient.

700 band, antennas 2 and 3 are used. It is seen that all the antenna elements show isolation above 10 dB in most of the covered frequency bands. The plot in Fig. 5(b) also shows good isolation (S_{12}, S_{13}, S_{14}, and S_{15}) of MIMO antennas with antenna 1 which make the proposed antenna system suitable for a wide range of applications. Fig. 5(c) shows the envelope reflection coefficient (ECC) between antennas 2 and 3 and between 4 and 5.

3. FABRICATION AND RESULTS

3.1. Fabricated MIMO Antenna

The fabricated MIMO antenna is shown in Fig. 6. Fabrication was done at Antenna Design Lab, SMVDU, Katra. Radiation pattern measurement was done inside an anechoic chamber, and the S-parameters were measured with Anritsu vector network analyzer (MS2038C) shown in Fig. 7. The vector network analyser (VNA) was calibrated using Short, Open load and Through (SOLT) method. The dynamic range of the measurement setup was 85 to 100 dB in 5 kHz to 18 GHz, and the noise floor was −60 dB. The intermediate frequency bandwidth used for the vector network analyser (VNA) was 10 kHz. N-type coaxial cable was used to connect SMA adapter and antenna to the VNA ports. The cable was compensated by calibrating the chamber using full S_{21} caliberation available in VNA.

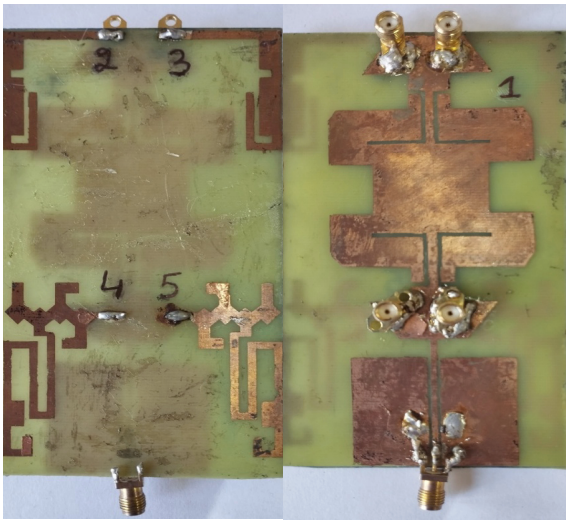

(a) (b)

Figure 6. Antenna prototype. (a) Top view and (b) bottom view.

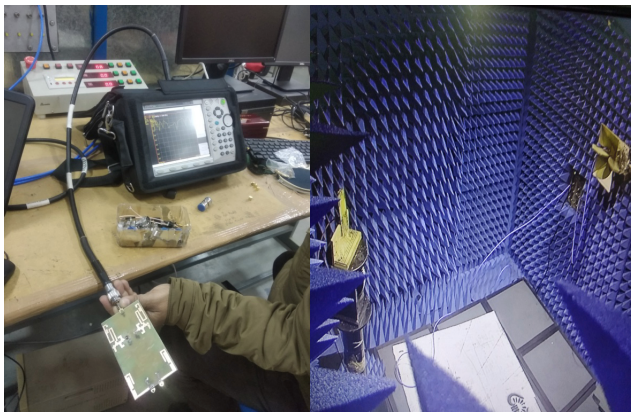

(a) (b)

Figure 7. Measurement setup. (a) S-parameter measurement by Vector Network Analyser (VNA), (b) radiation pattern measurement in an anechoic chamber.

3.2. S-Parameters of Fabricated Antenna

Simulated and measured results of antenna 1 (S_{11}), antenna 2 and 3 (S_{22}, S_{33}), and antenna 4 and 5 (S_{44}, S_{55}) are presented in Fig. 8, Fig. 9(a), and Fig. 9(b), respectively. It is observed that multiple wireless bands are covered by the proposed antenna for latest wireless applications. Simulated and measured isolation values are presented in Fig. 10. The measured S_{23} and S_{45} are less than −10 dB level in the desired frequency range. Slight variations between simulated and experimental results are because of minor changes in port impedances during fabrication.

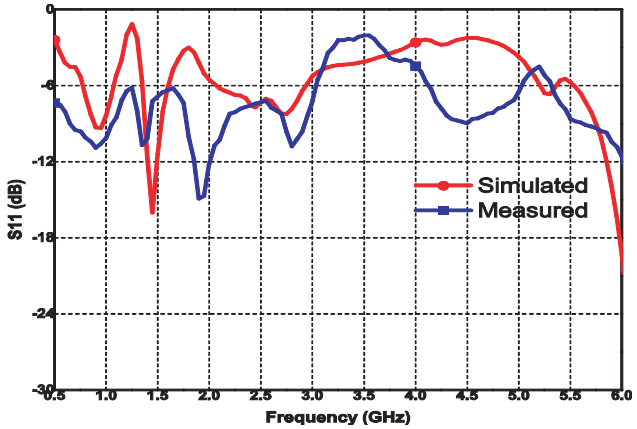

Figure 8. Simulated and measured reflection coefficient (Antenna 1).

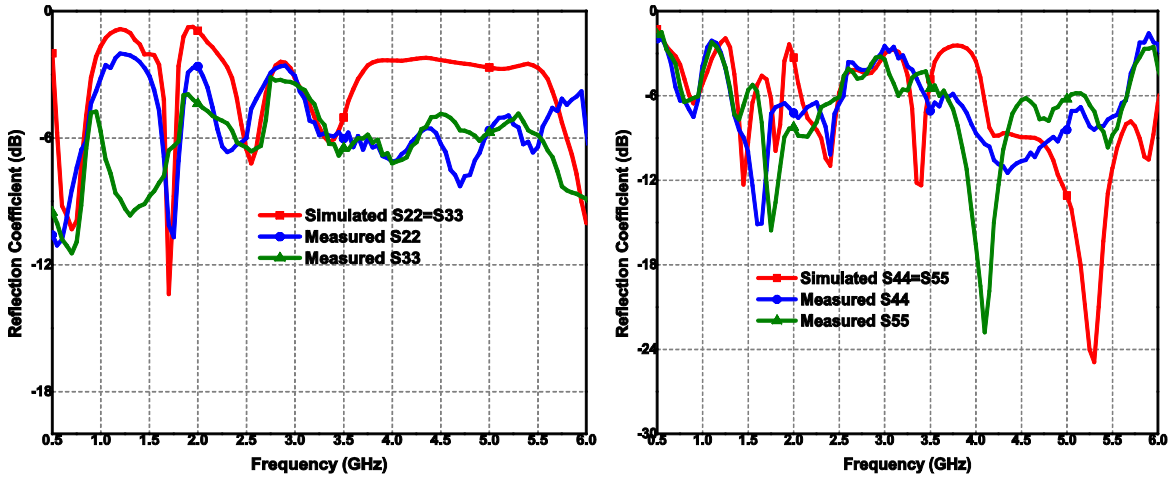

(a) (b)

Figure 9. Simulation and measured reflection coefficient. (a) Antennas 2 and 3 and (b) Antennas 4 and 5.

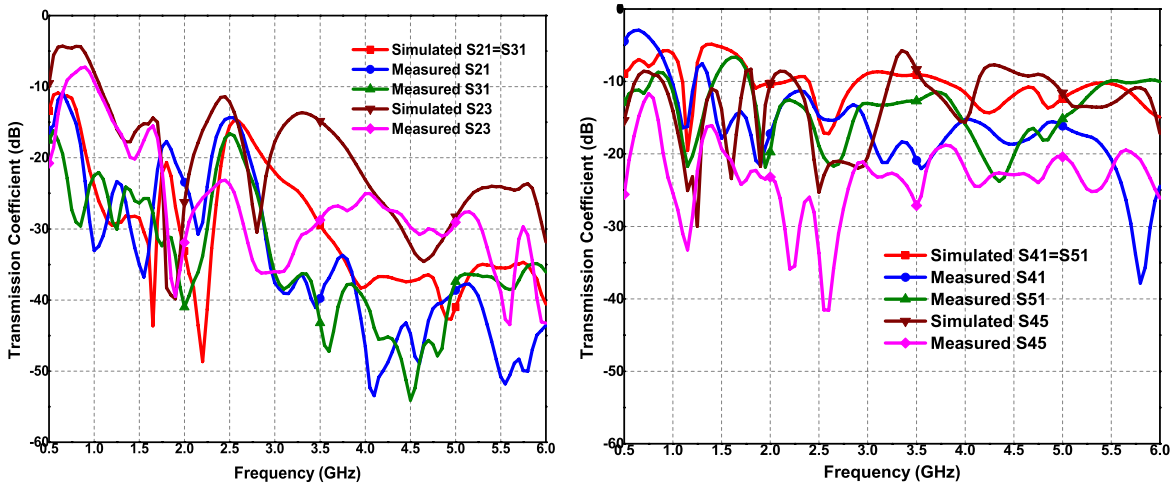

(a) (b)

Figure 10. Simulated and Measured Isolation parameters. (a) Antennas 2 and 3 and (b) Antennas 4 and 5.

3.3. Measured Radiation Parameters

3.3.1. Realized Gain

The 3-D radiation pattern was measured by keeping the angular step size of 22.5°. Table 2 gives the simulated and experimental values of realized gains of antenna 1 at 0.9 GHz and 2.4 GHz, antennas 2 and 3 at 0.8 GHz, and antennas 4 and 5 at 0.9 GHz and 5.8 GHz.

Table 2. Realized gain of the antenna.

Realized Gain (dBi)								
Results	**Antenna 1**		**Antenna 2**	**Antenna 3**	**Antenna 4**		**Antenna 5**	
	Frequency (GHz)		**Frequency (GHz)**	**Frequency (GHz)**	**Frequency (GHz)**		**Frequency (GHz)**	
	0.9	**2.4**	**0.8**	**0.8**	**0.9**	**5.8**	**0.9**	**5.8**
Simulated	−5.69	0.1441	−4.651	−4.651	−3.105	3.188	−3.105	3.188
Measured	−1.64	−0.214	−3.54	−0.63	−4.33	−0.13	−4.09	−0.06

3.3.2. Radiation Pattern and Directivity

The normalized measured 2-D radiation in the θ and φ-plane are given in Figs. 11 to 14. Figs. 11(a) and 11(b) show the pattern of antenna 1 at 900 MHz and 2.4 GHz, respectively. Antenna shows omnidirectional pattern. Fig. 12(a) and 12(b) show the pattern of antenna 2 and 3 respectively at 800 MHz. Fig. 13(a) and 13(b) show the pattern of antenna 4 and antenna 5 respectively at 900 MHz. Fig. 14(a) and 14(b) show the radiation characteristics of antenna 4 and 5 respectively at 5.8 GHz. Table 3 shows the measured and simulated values of directivity.

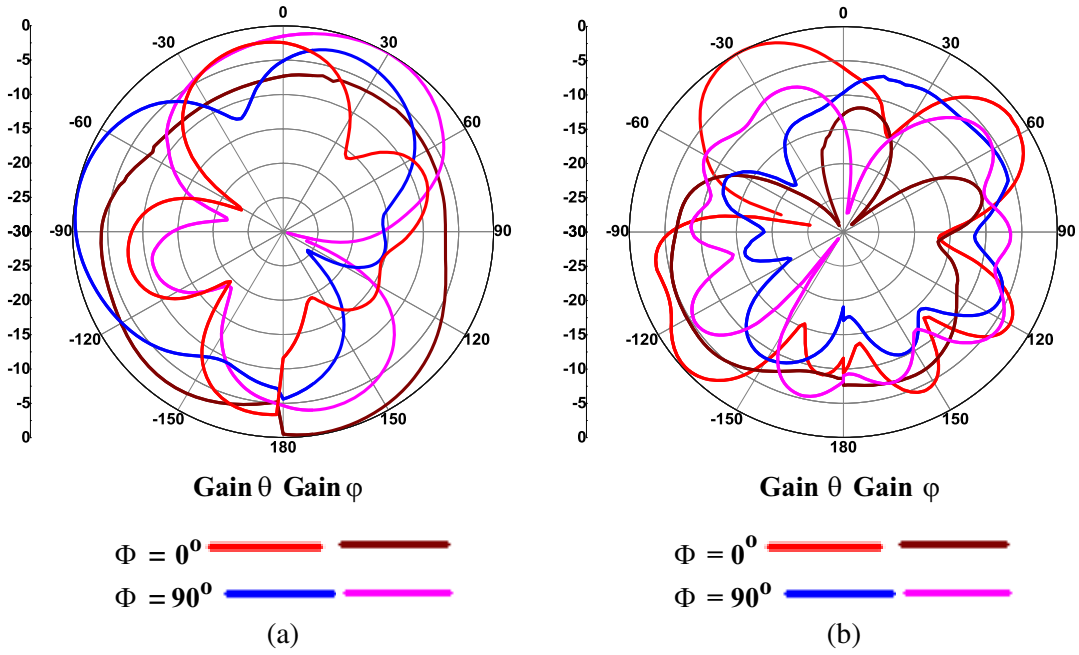

Figure 11. Measured antenna radiation pattern (antenna 1) at (a) 900 and (b) 2400 MHz.

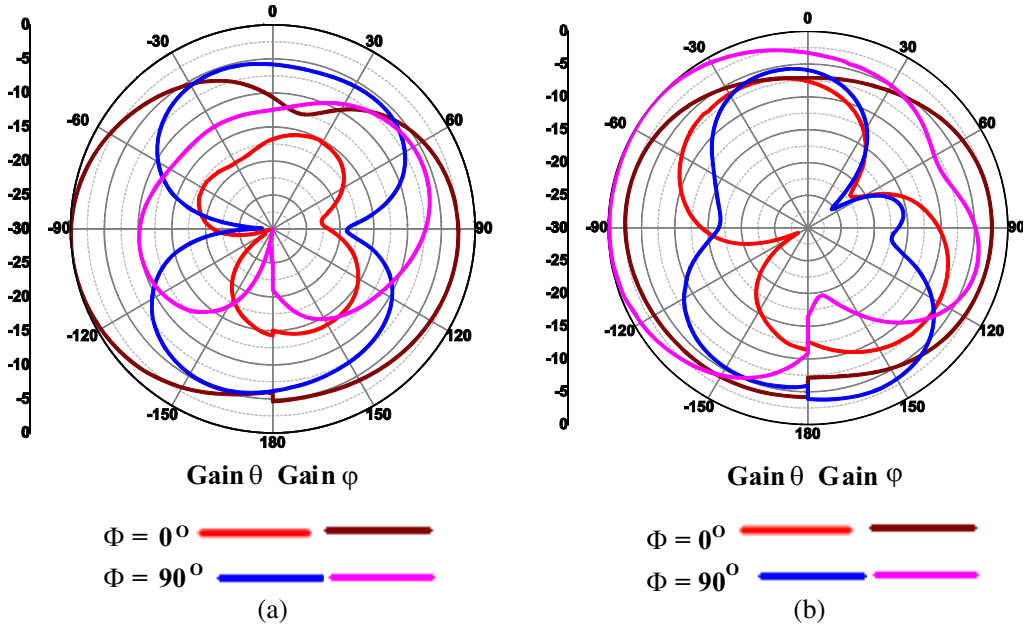

Figure 12. Measured antenna radiation pattern (a) antenna 2 and (b) antenna 3 at 800 MHz.

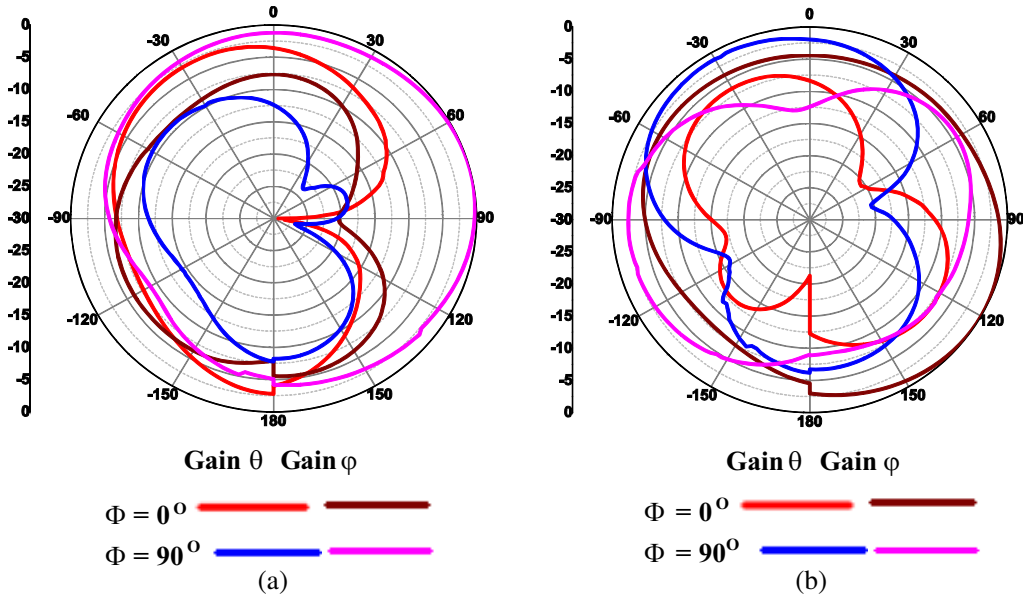

Figure 13. Measured antenna radiation pattern (a) antenna 4 and (b) antenna 5 at 900 MHz.

Table 3. Directivity.

Directivity (dBi)								
Results	Antenna 1		Antenna 2	Antenna 3	Antenna 4		Antenna 5	
	Frequency (GHz)		Frequency (GHz)	Frequency (GHz)	Frequency (GHz)		Frequency (GHz)	
	0.9	2.4	0.8	0.8	0.9	5.8	0.9	5.8
Simulated	2.213	4.637	2.396	2.396	3.115	6.988	3.115	6.988
Measured	2.137	4.622	2.388	2.1924	2.886	6.6046	2.9041	6.7352

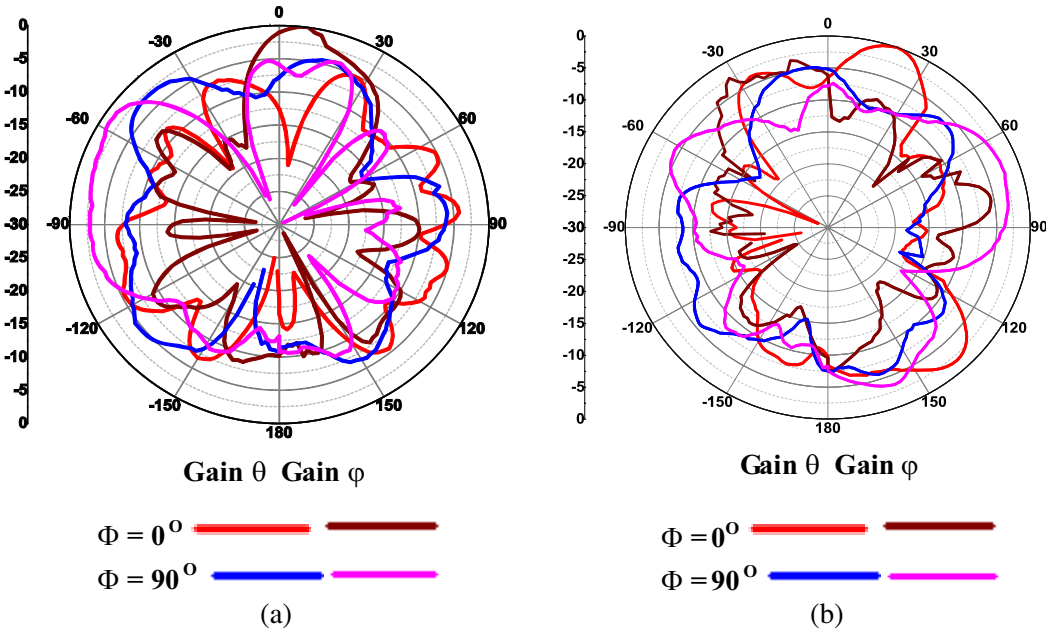

Figure 14. Measured antenna radiation pattern (a) antenna 4 and (b) antenna 5 at 5.8 GHz.

4. MIMO PARAMETERS

To implement the antennas in MIMO configuration, the envelope correlation coefficient between them should be less than 0.5 [38] for minimum interaction between them. The envelope correlation coefficient between antennas 2 and 3 and antennas 4 and 5 at some of the frequencies is measured from 3-D pattern using the equation given below:

$$\text{Envelope Correlation Coefficient} = \frac{\left|\iint_{4\pi} \overrightarrow{F_i}(\theta,\varphi) \cdot \overrightarrow{F_j}(\theta,\varphi)^* \, \partial\Omega\right|^2}{\iint_{4\pi} \left|\overrightarrow{F_i}(\theta,\varphi)\right|^2 \partial\Omega \iint_{4\pi} \left|\overrightarrow{F_j}(\theta,\varphi)\right|^2 \partial\Omega} \tag{2}$$

where $\cdot$, $\overrightarrow{F_i}(\theta,\varphi)$ and $\overrightarrow{F_j}(\theta,\varphi)$ denote the Hermitian multiplication and radiation patterns of antennas i and j, respectively [38]. The simulated and measured envelope correlation coefficients between antennas 2 and 3 at 0.8 GHz and between antennas 4 and 5 at 0.9 GHz are given in Table 4. The simulated and measured values are below 0.5 which make them suitable for MIMO implementation. The slight variations between simulated and experimental results are due to limitations in the experimental setup like bigger step size. To minimize the error, the step size has to be decreased which in turn will make the measurement more complex.

Table 4. Envelope correlation coefficient.

Between Antenna 2 & 3			Between Antenna 4 & 5		
Frequency (GHz)	Simulated	Measured	Frequency (GHz)	Simulated	Measured
0.8	0.1068	0.1640	0.9	0.0460	0.0243

5. STATE-OF-ART-COMPARISON

Table 5 gives the state-of-art-comparison of the proposed work with some recently presented works to show its wide usability in various wireless communication applications like CR, LTE, IoT, RFID, etc. for

small devices. The table shows that the proposed MIMO antenna supports multiple wireless standards keeping in view the size constraints.

Table 5. State-of-the-art comparison.

Ref.	Dimensions (mm^3)	Range of Sensing Frequency (GHz)	Communication Frequency bands covered (GHz)	Implementation
[26]	$68 \times 51 \times 1.6$	2.63 to 3.7	2.63 to 3.7	SISO
[27]	$11.5 \times 8.4 \times 1.6$	2 to 3	2.39 to 2.62, 2.69 to 3.0	SISO
[29]	$40 \times 36 \times 1.66$	3 to 11	5 to 6	SISO
[30]	$21 \times 9 \times 0.8$	2.8 to 10.4	3.2 to 4.5, 4.3 to 7.8, 7.9 to 11.2	SISO
[31]	$80 \times 65 \times 1.5$	2 to 5.5	2.6 to 2.7	SISO
[33]	$63 \times 63 \times 1.52$	3.4 to 8	5.7 to 5.4	SISO
[39]	$45 \times 45 \times 0.8$	1.52 to 2.75	1.54 to 2.28, 2.28 to 2.85	SISO
[40]	$65 \times 120 \times 1.56$	0.7 to 3	0.78 to 1.2, 1.49 to 1.76, 0.61 to 0.92, 1.21 to 1.43, 0.94 to 1.35	MIMO
Proposed	$65 \times 120 \times 1.6$	0.78 to 1.07, 1.36 to 1.6, 2.07 to 2.93, 5.21 to 5.36, 5.54 to 6.	559 to 828, 1.68 to 1.77, 2.48 to 2.63, 3.3 to 3.4, 5.79 to 6, 854 to 958, 1.38 to 1.56, 1.75 to 1.87, 2.08 to 2.49, 3.29 to 3.47, 4.09 to 6	MIMO

6. CONCLUSION

A compact MIMO antenna design is proposed covering multiple bands for LTE 700 band, CR, RFID, and IoT applications. Due to compact size, it can be used in latest handheld devices where size is an important design constraint. The antenna elements show less mutual coupling, and the ECC between them is below 0.5. The antenna system covers almost all of the sub-6 GHz bands making it suitable for 5G New Radio (NR) applications. It can also be interfaced with various modules like Wi-Fi, GSM, RFID, etc. for tracking, detection and biomedical applications like health monitoring, etc.

REFERENCES

1. Shereen, M. K., M. I. Khattak, and J. Nebhen, "A review of achieving frequency reconfiguration through switching in microstrip patch antennas for future 5G applications," *Alexandria Engineering Journal*, Vol. 61, No. 1, 29–40, 2022.
2. Kim, G. and K. Sangkil, "Design and analysis of dual polarized broadband microstrip patch antenna for 5G mm wave antenna module on FR4 substrate," *IEEE Access*, Vol. 9, 64306–64316, 2021.
3. Kumar, G. and K. P. Ray, *Broadband Microstrip Antennas*, Artech House, London, U.K., 2003.
4. Haykin, S., "Cognitive radio: Brain-empowered wireless communications," *IEEE Journal on Selected Areas in Communications*, Vol. 23, No. 2, 201–220, 2005.
5. Tawk, Y., J. Costantine, and C. Christodoulou, *Antenna Design for Cognitive Radio*, Artech House Boston, USA, 2016.
6. De Flaviis, F., L. Jofre, J. Romeu, and A. Grau, "Multiantenna systems for MIMO communications," *Synthesis Lectures on Antennas*, Vol. 3, No. 1, 1–250, 2008.
7. Varzakas, P., "Estimation of radio capacity of a spread spectrum cognitive radio rayleigh fading system," *ACM Proceedings of the 17th Pan-Hellenic Conference on Informatics with International Participation*, 63–66, 2013.
8. Bakulin, M. G., V. B. Kreindelin, and D. Y. Pankratov, "Analysis of the capacity of MIMO channel in fading conditions," *2018 Systems of Signal Synchronization, Generating and Processing in Telecommunications (SYNCHROINFO)*, 1–6, 2018.
9. Chitra, M. P., S. Divya, M. Premkumar, V. Tamilselvi, and N. Karthika, "MIMO cognitive radio capacity in flat fading channel," *2017 Third International Conference on Science Technology Engineering & Management (ICONSTEM)*, 915–919, 2017.
10. Cheng, B. and Z. Du, "Dual polarization MIMO antenna for 5G mobile phone applications," *IEEE Transactions on Antennas and Propagation*, Vol. 69, No. 7, 4160–4165, 2020.
11. Chen, Y. S. and C. P. Chang, "Design of a four-element multiple-input-multiple-output antenna for compact long-term evolution small-cell base stations," *IET Microwaves, Antennas & Propagation*, Vol. 10, No. 4, 385–392, 2016.
12. Chen, W. S. and K. H. Lai, "Compact design of MIMO antennas for LTE 700 application," *2015 IEEE International Symposium on Antennas and Propagation & USNC/URSI National Radio Science Meeting*, 1148–1149, 2015.
13. Singh, H. S., G. K. Pandey, P. K. Bharti, and M. K. Meshram, "Compact printed diversity antenna for LTE700/GSM1700/1800/UMTS/Wi-Fi/Bluetooth/LTE2300/2500 applications for slim mobile handsets," *Progress In Electromagnetics Research C*, Vol. 56, 83–91, 2015.
14. Naser, A. A., K. Sayidmarie, and J. S. Aziz, "Compact high isolation meandered-line PIFA antenna for LTE (band-class-13) handset applications," *Progress In Electromagnetics Research C*, Vol. 67, 153–164, 2016.
15. Jan, M. A., D. N. Aloi, and M. S. Sharawi, "A 2×1 compact dual band MIMO antenna system for wireless handheld terminals," *2012 IEEE Radio and Wireless Symposium*, 23–26, 2012.
16. Ikram, M., R. Hussain, A. Ghalib, and M. S. Sharawi, "Compact 4-element MIMO antenna with isolation enhancement for 4G LTE terminals," *2016 IEEE International Symposium on Antennas and Propagation (APSURSI)*, 535–536, 2016.
17. Ikram, M. and M. S. Sharawi, "Compact 10-element monopole based MIMO antenna system for 4G mobile phones," *2016 16th Mediterranean Microwave Symposium (MMS)*, 1–2, 2016.
18. Shoaib, S., I. Shoaib, N. Shoaib, X. Chen, and C. Parini, "Compact and printed MIMO antennas for 2G/3G and 4G-LTE mobile tablets," *2015 IEEE-APS Topical Conference on Antennas and Propagation in Wireless Communications (APWC)*, 674–677, 2015.
19. Li, S., L. Da Xu, and S. Zhao, "The internet of things: A survey," *Information Systems Frontiers*, 243–259, 2015.
20. Zaman, M. R., R. Azim, N. Misran, M. F. Asillam, and T. Islam, "Development of a semielliptical partial ground plane antenna for RFID and GSM-900," *International Journal of Antennas and*

Propagation, 2014.

21. Bukhari, B., C. Singh, K. R. Jha, and S. K. Sharma, "Planar MIMO antennas for IoT and CR applications," *2017 IEEE Applied Electromagnetics Conference (AEMC)*, 1–2, 2017.
22. Bashir, U., K. R. Jha, G. Mishra, G. Singh, and S. K. Sharma, "Octahedron-shaped linearly polarized antenna for multistandard services including RFID and IoT," *IEEE Transactions on Antennas and Propagation*, Vol. 65, No. 7, 3364–3373, 2017.
23. Ebrahimi, E. and P. S. Hall, "A dual port wide-narrowband antenna for cognitive radio," *2009 3rd European Conference on Antennas and Propagation*, 809–812, 2009.
24. Al-Husseini, M., Y. Tawk, C. G. Christodoulou, K. Y. Kabalan, and A. El Hajj, "A reconfigurable cognitive radio antenna design," *2010 IEEE Antennas and Propagation Society International Symposium*, 1–4, 2010.
25. Tawk, Y., J. Costantine, K. Avery, and C. G. Christodoulou, "Implementation of a cognitive radio front-end using rotatable controlled reconfigurable antennas," *IEEE Transactions on Antennas and Propagation*, Vol. 59, No. 5, 1773–1778, 2011.
26. Mansoul, A., F. Ghanem, M. R. Hamid, and M. Trabelsi, "A selective frequency-reconfigurable antenna for cognitive radio applications," *IEEE Antennas and Wireless Propagation Letters*, Vol. 13, 515–518, 2014.
27. Cao, Y., S. W. Cheung, X. L. Sun, and T. I. Yuk, "Frequency-reconfigurable monopole antenna with wide tuning range for cognitive radio," *Microwave and Optical Technology Letters*, Vol. 56, No. 1, 145–152, 2014.
28. Zheng, S. H., X. Y. Liu, and M. M. Tentzeris, "A novel optically controlled reconfigurable antenna for cognitive radio systems," *2014 IEEE Antennas and Propagation Society International Symposium (APSURSI)*, 1246–1247, 2014.
29. Erfani, E., J. Nourinia, C. Ghobadi, M. Niroo-Jazi, and T. A. Denidni, "Design and implementation of an integrated UWB/reconfigurable-slot antenna for cognitive radio applications," *IEEE Antennas and Wireless Propagation Letters*, Vol. 11, 77–80, 2012.
30. Srivastava, G., A. Mohan, and A. Chakrabarty, "Compact reconfigurable UWB slot antenna for cognitive radio applications," *IEEE Antennas and Wireless Propagation Letters*, Vol. 16, 1139–1142, 2016.
31. Nachouane, H., A. Najid, A. Tribak, and F. Riouch, "Dual port antenna combining sensing and communication tasks for cognitive radio," *International Journal of Electronics and Telecommunications*, Vol. 62, No. 2, 121–127, 2016.
32. Hu, Z. H., P. S. Hall, and P. Gardner, "Reconfigurable dipole-chassis antennas for small terminal MIMO applications," *Electronics Letters*, Vol. 47, No. 17, 953–955, 2011.
33. Chacko, B. P., G. Augustin, and T. A. Denidni, "Electronically reconfigurable uniplanar antenna with polarization diversity for cognitive radio applications," *IEEE Antennas and Wireless Propagation Letters*, Vol. 14, 213–216, 2015.
34. Cheng, S. P. and K. H. Lin, "A reconfigurable monopole MIMO antenna with wideband sensing capability for cognitive radio using varactor diodes," *2015 IEEE International Symposium on Antennas and Propagation & USNC/URSI National Radio Science Meeting*, 2233–2234, 2015.
35. Tawk, Y., F. Ayoub, C. G. Christodoulou, and J. Costantine, "A MIMO cognitive radio antenna system," *2013 IEEE Antennas and Propagation Society International Symposium (APSURSI)*, 572–573, 2013.
36. Hussain, R. and M. S. Sharawi, "Integrated reconfigurable multiple-input-multiple-output antenna system with an ultra-wideband sensing antenna for cognitive radio platforms," *IET Microwaves, Antennas & Propagation*, Vol. 9, No. 9, 940–947, 2015.
37. *Truncated Cube — From Wolfram MathWorld 2017*, http://mathworld.wolfram.com/TruncatedTetrahedron.html, Accessed Dec. 11, 2021.
38. Jha, K. R. and S. K. Sharma, "Combination of frequency agile and quasi-elliptical planar monopole antennas in MIMO implementations for handheld devices," *IEEE Antennas Propagation Mag.*, Vol. 60, 118–131, 2018.

39. Fakharian, M. M., P. Rezaei, and A. A. Orouji, "A novel slot antenna with reconfigurable meander-slot DGS for cognitive radio applications," *Applied Computational Electromagnetics Society Journal (ACES)*, Vol. 30, No. 7, 748–753, 2015.
40. Hussain, R. and M. S. Sharawi, "Planar four-element frequency agile MIMO antenna system with chassis mode reconfigurability," *Microwave and Optical Technology Letters*, Vol. 57, No. 8, 1933–1938, 2015.